GEOLOGY

Critical transitions in Chinese dunes during the past 12,000 years

Zhiwei Xu[1]*, Joseph A. Mason[2], Chi Xu[3], Shuangwen Yi[1], Sebastian Bathiany[4], Hezi Yizhaq[5], Yali Zhou[6], Jun Cheng[7], Milena Holmgren[8], Huayu Lu[1]

Dune systems can have alternative stable states that coexist under certain environmental conditions: a vegetated, stabilized state and a bare active state. This behavior implies the possibility of abrupt transitions from one state to another in response to gradual environmental change. Here, we synthesize stratigraphic records covering 12,000 years of dynamics of this system at 144 localities across three dune fields in northern China. We find side-by-side coexistence of active and stabilized states, and occasional sharp shifts in time between those contrasting states. Those shifts occur asynchronously despite the fact that the entire landscape has been subject to the same gradual changes in monsoon rainfall and other conditions. At larger scale, the spatial heterogeneity in dune dynamics averages out to produce relatively smooth change. However, our results do show different paths of recovery and collapse of vegetation at system-wide scales, implying that hysteretic behavior occurs in spatially extended systems.

INTRODUCTION

Increasing evidence has shown that many complex climatic (*1*), ecological (*2*), and geomorphological (*3*) systems have alternative stable states. Gradual forcing or small perturbations can trigger critical transitions (or tipping points) between alternative stable states in these systems, which often proceed nonlinearly with drastic changes of system states in relatively short time periods (*2*). It has been proposed that dune systems may also have these alternative stable states, as seen from the observation that bare, active dunes can coexist with vegetation-stabilized dunes under the same climatic conditions and in the same geographic area (*4*). Recent biophysical models (*5*, *6*) indicate that critical transitions can occur between these alternative states. For example, a vegetation-stabilized dune can transition to an active state induced by reduced precipitation and will not be stabilized again unless precipitation is elevated to a much higher level than the initial threshold needed for dune activation. In the range between thresholds for activation and stabilization, dunes in both active and stabilized states can coexist. It remains unknown whether this type of dune system behavior also occurs in nature over a wide range of temporal and spatial scales.

One exceptional case in which a critical transition from a vegetated state to a desert state has been described at very large scales is the loss of relatively dense vegetation over the western Sahara region around 5 thousand years (ka) ago (*7*), attributed to strong positive feedbacks between vegetation and precipitation (*8*). Further studies concluded that the transition was time transgressive (*9*) and more gradual in central Sahara (*10*) and emphasized the importance of local feedbacks, spatial heterogeneity (*11*), and climate variability (*12*, *13*) in understanding the large-scale transition. Local conditions (*14*), ecological interactions (*15*), and pulse dynamics (*16*) have proved to be very important to understand critical transitions in arid regions and in ecosystems in general.

Here, we report geological evidence for critical transitions between active and stabilized states—controlled by vegetation—over the past 12,000 years in three major semiarid dune fields of northern China (Mu Us, Otindag, and Horqin dune fields) where present dunes display bistability (Fig. 1). This bistability is usually characterized by active barchans and transverse dunes coexisting with vegetated patches that are mostly stabilized parabolic dunes. In this region with a modern annual precipitation of 200 to 450 mm (increasing from northwest to southeast), changes in dune activity are influenced by the Asian monsoon climate (*17*, *18*). Monsoon precipitation increased from the Early to Middle Holocene and decreased during the Late Holocene according to proxy records (*19*–*21*). Dune stabilization in response to increasing monsoon precipitation, and reactivation as precipitation later declined, are indicated by many dune stratigraphic records from these dune fields (data file S1) (*17*, *22*–*27*). However, it is also apparent that despite similar climatic forcing, dune strata and the timing and pattern of shifts in dune activity are quite varied and sometimes difficult to correlate among individual sites, even in the same dune field (*24*–*26*). This heterogeneity of dune records has also been recognized in many other dune fields globally (*28*–*31*). Meanwhile, the increasingly large number of well-dated dune field records allows an integrated approach (*32*), providing a comprehensive picture of long-term dune field evolution and new insight on the past occurrence of bistability and hysteresis in response to environmental change. In this study, we analyze a large dataset of dune stratigraphic sections with independent age controls in the dune fields of northern China (data file S2) and investigate possible transitions at scales from local (individual study sites) to regional (across all three dune fields) during the past 12,000 years.

RESULTS

The dune stratigraphic sections in the three dune fields are characterized by alternations between aeolian sand layers and paleosols, recording changes between active and stabilized states of the dunes

[1]School of Geography and Ocean Science, Nanjing University, Nanjing 210023, China. [2]Department of Geography, University of Wisconsin–Madison, WI 53706, USA. [3]School of Life Sciences, Nanjing University, Nanjing 210023, China. [4]Department of Aquatic Ecology and Water Quality Management, Wageningen University, NL-6700 AA Wageningen, Netherlands. [5]Department of Solar Energy and Environmental Physics, Blaustein Institutes for Desert Research, Ben-Gurion University of the Negev, Sede Boqer Campus, 84990, Israel. [6]School of Geography and Tourism, Shaanxi Normal University, Xi'an 710119, China. [7]Polar Climate System and Global Change Laboratory, Nanjing University of Information Science and Technology, Nanjing 210044, China. [8]Resource Ecology Group, Wageningen University, NL-6700 AA Wageningen, Netherlands.
*Corresponding author. Email: zhiweixu@nju.edu.cn

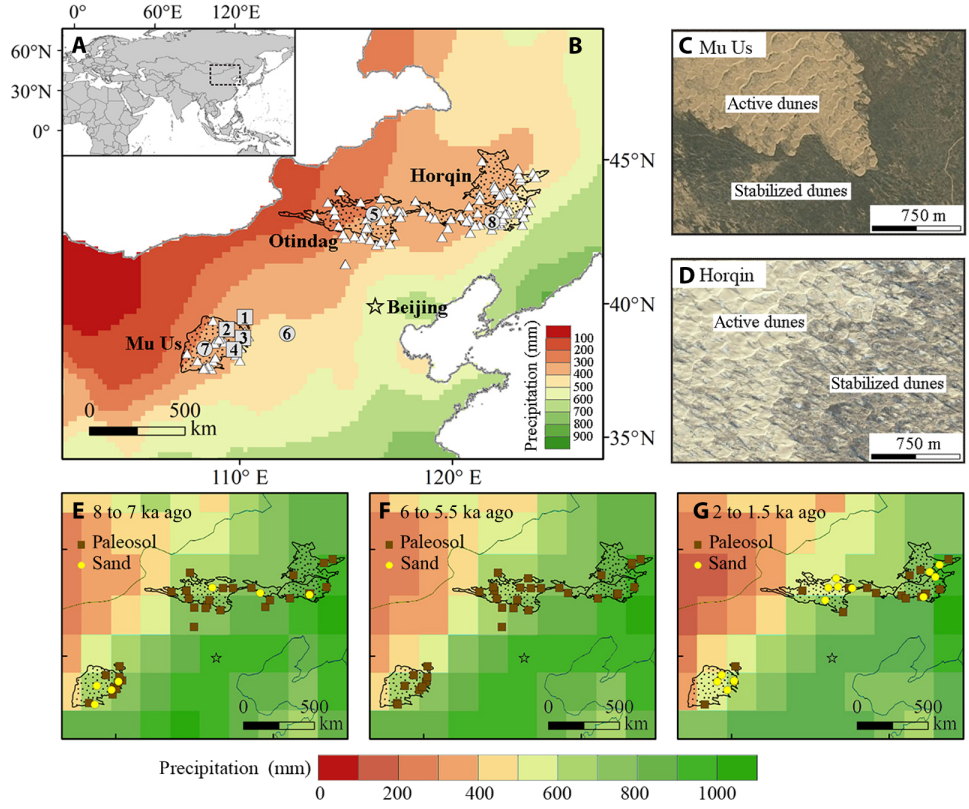

Fig. 1. Coexisting active and stabilized dunes in northern China at the present and in the geological past. (**A**) Geographic location of dune fields in northern China marked by the dashed box. (**B**) Locations of the Mu Us, Otindag, and Horqin dune fields. Precipitation in these dune fields is dominated by the Asian summer monsoon from the southeast, and strong wind predominantly comes from the northwest by the East Asian winter monsoon (EAWM). The triangles represent the studied dune stratigraphic sections. 1, SGD (Shigadu); 2, TK (Tuke); 3, JJ (Jinjie); 4, ZBT (Zhenbeitai); 5, Dali Lake; 6, Gonghai Lake. Markers 7 and 8 indicate the locations for (C) and (D). (**C** and **D**) Examples of active and stabilized dunes coexisting in the Mu Us and Horqin dune field, respectively. High reflectance indicates bare sand dunes, while dark color reflects dense vegetation patches where the dunes are stabilized. North is toward the top of the satellite images from Google Earth. (**E** to **G**) Time slices showing the spatial distribution pattern of dune activity at individual sites during 8 to 7, 6 to 5.5, and 2 to 1.5 ka ago, respectively. The brown/yellow symbols indicate stabilized/active state of the dunes. Rainfall data in (A) are based on modern observations, while precipitation in (E to G) is simulated by the Earth system model MPI-ESM. See fig. S2 for other time intervals since 12 ka ago, and data file S3 for sites recording sand deposition or soil development during each interval.

at individual sites (fig. S1). Paleosols correspond to intervals of local dune stability, separating sand deposited when aeolian sand was largely mobile at a given site. As demonstrated in previous studies (*23*, *25*), the paleosols in the dune fields of northern China are often recognized as accretionary soils, in that accumulation of sediment on the vegetated surface often occurs even during the period of soil formation. They can be clearly distinguished from aeolian sand layers in the field by their distinct texture, color, and grain size, an interpretation supported by laboratory measurements showing higher magnetic susceptibility in the paleosols (Fig. 2) and other sedimentary analysis (*23*, *25*).

The exact timing of changes in dune state at individual sites can be determined by numerical dating and, especially, by the optically stimulated luminescence (OSL) dating technique that has been used widely in recent years to date dune records. In this study, the OSL dating applied in most dune sections constrained the timing of aeolian sand deposition and, less directly, the ages of paleosols (see Materials and Methods). After a careful site-specific reconstruction of temporal changes in dune activity at individual sites, the cluster of multiple well-dated dune records (Fig. 2A) reveals the temporal pattern of dune field activity during the past 12,000 years and substantial differences in dune state shifts between individual sites. These clearly recorded alternations in dune state did not occur synchronously at the scale of the whole study region, individual dune fields, or even local areas within a dune field. Contrasting dune states recorded by either accumulative or discontinuous sections are easily found coexisting at the same time. In four accumulative sections from the Mu Us dune field (Fig. 2B), in close proximity to each other and with similar modern annual precipitation and sedimentation rate, a mostly active state during the Early Holocene (11.5 to 8 ka ago) is recorded by aeolian sand deposition. A subsequent major stabilization phase is indicated by a paleosol that formed during the Middle Holocene (8 to 4 ka ago), with reactivation in the Late Holocene (4 ka ago to present). Frequency distributions of the magnetic susceptibility data at each site indicate bimodal patterns of high and low values, reflecting transitions between active and stabilized states, with limited occurrence of intermediate conditions.

However, the exact timing of these state shifts is substantially different between these four sites (Fig. 2B). The SGD (Shigadu) site remained stabilized through part of the Late Holocene, as indicated by soil development continuing until 2 ka ago, while active sand accumulation began much earlier at the adjacent TK (Tuke) site. Both ZBT (Zhenbeitai) and JJ (Jinjie) sites are located in the southeast part of the Mu Us dune field in similar conditions, but the transition

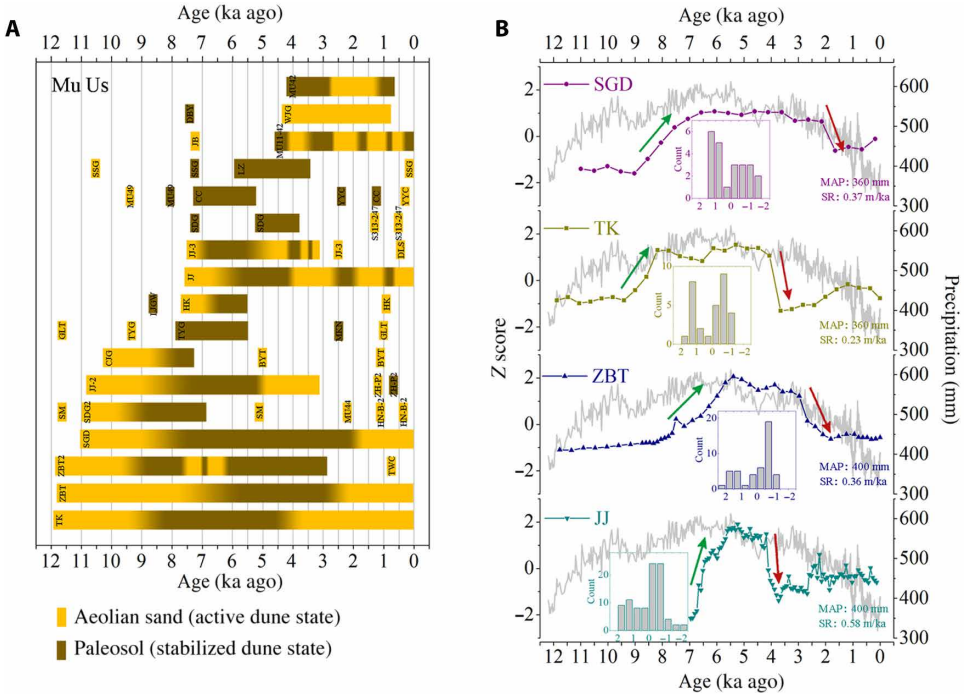

Fig. 2. Critical transitions in dune activity at individual sites in response to monsoon precipitation change. (**A**) Temporal pattern of the shifts in dune activity at individual sites revealed by a cluster of study sites from the Mu Us dune field as an example. The temporal phases of active dune state (indicated by aeolian sand deposit) and stabilized dune state (indicated by the paleosol) are illustrated by yellow and brown columns (or bars), respectively. The name of the section at each site is labeled on the left of each column or on the bar. The short bar refers to discontinuous site, while the long column is based on the accumulative site. (**B**) Changes in dune activity at four representative accumulative sites (SGD, TK, ZBT, and JJ) in the Mu Us dune field indicated by magnetic susceptibility of the sediments. Changes in monsoon precipitation (gray line) are reconstructed on the basis of the Gonghai Lake pollen record (*21*). The magnetic susceptibility data were normalized to the standard *Z* score: $Z = (X - V)/SD$; here, *X* is the original value, and *V* and SD are the averaged value and standard deviation of the time series. High/low values of the normalized *Z* score represent high/low magnetic susceptibility, indicating the shifts between active and stabilized dune states. The green/red arrow indicates the transition from active/stabilized to stabilized/active state, with different timing at each site. Note the asymmetry between the stabilization and activation processes (further discussed in the main text). The column shows the frequency distribution of the normalized *Z* score of magnetic susceptibility. Modern annual precipitation (MAP) and sedimentation rate (SR) at each site are labeled in the figure. The MAP at the Gonghai Lake is ~445 mm, approximate to that of the southeast margin of the dune fields. ZBT data were previously published by Lu *et al.* (*20*). The original data for the JJ site was from Ma *et al.* (*59*).

from a stabilized to an active state at the JJ site occurred at 4 ka ago, while the ZBT site remained stabilized by vegetation until much later. The shifts to an active condition (S/A transition; indicated by red arrows) at the JJ and TK sites were abrupt, but the ZBT site initially experienced more limited, possibly intermittent activity before settling into a fully active state after 3 ka ago. The average time required for the Late Holocene S/A transition recorded by these sites is about 500 years. Compared to that, the transition from an active to a stabilized state (A/S transition; indicated by green arrows) at these sites during the Early to Middle Holocene appears slower, taking place over 1000 to 2000 years, possibly reflecting the additional time required for recognizable soil formation on a stabilized dune. However, the timing of the earlier A/S transition still varied between sites: It occurred during 9 to 7 ka ago at the SGD site, 9 to 8 ka ago at the TK site, 8 to 6 ka ago at the ZBT site, and 7 to 6 ka ago at the JJ site despite the similar monsoon climate.

All four of these sites were in a stabilized state during or just after the time of peak Holocene precipitation as shown in Fig. 2B around 6 ka ago. At all sites, however, the Early to Middle Holocene shifts toward stability and soil development occurred after precipitation rose in the Early Holocene. Although the time required for soil formation may have increased the apparent duration of the A/S transition at the four sites, the time lag between the change to a wetter climate and the A/S transition differs distinctly between sites, most likely reflecting different response times to monsoon change. Furthermore, the subsequent shifts back toward an active state do not closely track declining precipitation, again indicating nonlinear response to monsoon change and different time scales of response at individual sites.

The much larger set of discontinuous sites also demonstrates that adjacent sites can have contrasting dune states at the same time, clearly consistent with the long-term persistence of bistability. As illustrated by examples in Fig. 1 and fig. S2, most sites are characterized by the development of dark, sandy loam paleosols around 6 ka ago (Fig. 1F), when active sand deposition was rare. Before and after that relatively short interval around 6 ka ago, active dunes coexisted with stabilized dunes (Fig. 1, E and G, and fig. S2). Coexistence of active and stabilized dunes is demonstrated by nearly identical numerical ages dating sand deposition or soil formation at different sites (data file S2). The spatial pattern of mobility or stability at a given point in time does not follow any longitudinal or latitudinal pattern or display a clear relationship with any climatic gradient. Instead, active and stabilized dunes are recorded by sites quite close to each other, which must have always had similar climatic conditions. This coexistence of contrasting states can be explained using

the more continuous records available, as illustrated by the four accumulative sites in Fig. 2B, which show that each locality can have its own pathway of state shifts, from stabilized to active or vice versa.

Although active and stabilized dunes coexisted in these dune fields throughout much of the Holocene, their relative proportions have changed considerably over time (Fig. 3A). After widespread dune activity during the last glaciation (*18*, *33*), paleosol development reflecting stabilization is first recorded after about 11 ka ago, and thereafter, the proportion of vegetation-stabilized patches increased gradually. The greatest dominance of stabilized dunes occurred around 6 ka ago in the Middle Holocene (Fig. 1F), indicating largely vegetation-covered landscapes in the dune fields (*17*). Dune reactivation started after about 5 ka ago, and the proportion of vegetation-stabilized dunes decreased slowly, indicating an overall shift toward more activity during the Late Holocene.

Independent reconstructions (*21*) show that monsoon precipitation in northern China developed in a similar way to that of stabilized dunes: gradually increasing during the Early Holocene, reaching a maximum during the Middle Holocene, and decreasing during the Late Holocene (Fig. 3A). The MPI-ESM (Max Planck Institute Earth system model) and CCSM3 (Community Climate System Model, version 3.0) paleoclimate model simulations also show gradually decreasing rainfall after 5 ka ago (Fig. 3B), as a result of reduced insolation.

However, the proportion of sites with stabilized dunes increased substantially later than the increase in precipitation during the Early Holocene (before 8 ka ago) and did not follow exactly the same path as precipitation after 6 ka ago. The relationship between reconstructed precipitation and the relative proportion of sites with stabilized dunes displays clear evidence of hysteresis (Fig. 3D), with substantial divergence between the path to greater stability from 11 to 6 ka ago and the return to greater activity after 6 ka ago. At the four sites, the shift toward stability substantially lagged the Early Holocene rise in precipitation and, in some cases, preceded the major Late Holocene shift toward aridity (Fig. 2B).

DISCUSSION

Our results provide the first clear evidence of dune bistability persisting over geologic time scales, indicated by the coexistence of stabilized and active dunes throughout much of the past 12,000 years, under a wide range of reconstructed precipitation (300 to 600 mm). Data reported here demonstrate abrupt transitions in dune state at local scales. Both the apparently random spatial distributions of active and stabilized dunes at various times (Fig. 1 and fig. S2) and the different timing of abrupt transitions at nearby sites (Fig. 2) are consistent with bistability derived from the internal dynamics of the dune system, rather than spatial variation related to climatic gradients. At the regional scale (i.e., across all three dune fields), the large set of stratigraphic data we analyzed indicates gradual increases or decreases in the extent of dune stability or activity through the Holocene, rather than abrupt transitions (Fig. 3A). To reconcile our results over different spatial scales, we first discuss the mechanisms responsible for local-scale dune bistability and abrupt critical transitions and then propose an explanation for how this complex behavior contributes to the gradual response to external forcing observed across the dune fields at a larger scale.

Previous studies have proposed a variety of "ecogeomorphic" feedbacks between vegetation, water availability, and wind-driven

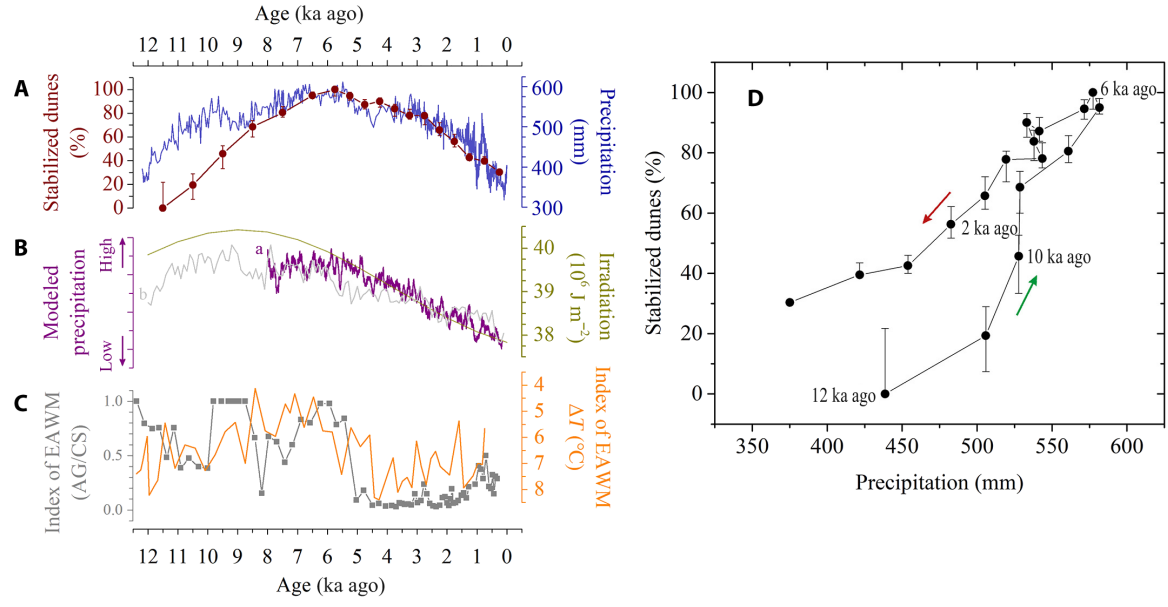

Fig. 3. Critical transitions of the entire Chinese dune fields to Holocene climate change. (**A**) Percentage of stabilized dune sites relative to all sites sampled in the dune fields over the past 12,000 years and annual precipitation in northern China over the same time period using the pollen-based reconstruction from Gonghai Lake (*21*). Error bars for percent stable represent 95% confidence interval based on 10,000 simulations incorporating errors of numerical ages. (**B**) Simulated precipitation change from the (a) MPI-ESM model and (b) CCSM3 model and boreal summer irradiation (*60*). (**C**) Index of the EAWM from a diatom record (*46*) and a marine record (*45*). The higher AG/CS (*A. granulate* and *C. stelligera*) represents stronger winter monsoon. The thermal gradient in the northern South China Sea represented by ΔT is strongly modulated by the EAWM, and the lower ΔT indicates stronger monsoon (*45*). (**D**) Plot of percent stabilized dune sites, relative to all the dune field sites sampled, against precipitation variation; note the hysteresis behavior. Precipitation data in (D) were based on the Gonghai Lake reconstruction. Notice that MAP at the Gonghai Lake is similar to the southeast margin of the dune fields but is about 150 mm higher than the average precipitation of the dune fields. Thus, the wide range of reconstructed precipitation (300 to 600 mm) refers in particular to the estimated annual precipitation at the southeast margin of the dune fields.

sand transportation (*4*, *34*–*36*), which over various time scales can lead to nonlinear and lagged responses to environmental change and, in some cases, the coexistence of active and stabilized dunes. Previous modeling studies (*5*, *6*) demonstrated the potential for bistability and hysteresis in response to environmental controls, arising simply from the interaction of fundamental processes that control dune activity across a wide range of wind strength, precipitation, and human disturbance. Only outside that range, for instance, in relatively wet climates without extreme winds or in very dry climates, will all dunes be in either stabilized or active states (monostability).

These predictions of bistability and other complex behavior are particularly plausible in the specific context of semiarid northern China. Given the relatively high population and widespread livestock grazing in these drylands, localized perturbations by weather extremes, fire, herbivores, or humans may activate the dunes at particular sites (*37*, *38*). The resulting active states can likely persist for some time because even relatively weak winds may mobilize sand and limit vegetation recovery on the bare sand, even if precipitation is high enough to maintain existing vegetation nearby. On the other hand, once dunes are stabilized by vegetation, an increase in wind strength cannot easily mobilize them because vegetation increases the surface roughness, reduces sand transport, and masks the land surface from wind erosion (*4*–*6*). Recently, Yizhaq and Ashkenazy (*39*) proposed that a model including the dynamics of both vegetation and biogenic soil crusts predicted intrinsic decadal to millennial oscillations of active and stabilized dunes under the same climatic conditions, potentially producing mosaics of active and stabilized patches as observed today and inferred from the geologic record. Other characteristics of the dune field environment in northern China suggest more complex or long-term feedbacks. The dune field vegetation is often shrub dominated, a context in which positive feedbacks that enhance local vegetation persistence have been identified [e.g., "islands of fertility" or "nurse plant effect"; (*40*)]. Higher vegetation cover allows for higher water infiltration and lower evaporation, promoting water availability for plants (*41*). Vegetation cover could also allow more accumulation of the dust frequently deposited in these dune fields, enhancing physical or biogenic crust development (*42*), increasing the resistance of soil surface to wind erosion (*43*), allowing greater retention of plant-available water, and making a long-stabilized dune increasingly less susceptible to reactivation (*44*). All of these feedbacks would favor persistence of stabilized dune patches despite widespread activation of surrounding areas in response to environmental change. Conversely, local vegetation disturbance and erosion of dust-enriched surface layers could lead to formation of active patches.

These local abrupt transitions between vegetated and bare sand states average at larger scales in a pattern of gradual change over time across all three dune fields (Fig. 3A). This pattern is consistent with earlier work explaining changes in dune activity as a response to variations in the Asian monsoon climate, especially rainfall and wind strength (*17*, *18*, *24*). The broad similarity between the temporal patterns of reconstructed and modeled precipitation and the proportion of stabilized dune sites (Fig. 3, A and B) seems readily explained by the positive effects of water availability on vegetation growth that directly affects dune stability. Wind strength also affects dune mobility (*4*, *5*), although its effect in the Holocene is not as clear as that of moisture. Evidence from sedimentary archives (*45*, *46*) shows that the intensity of the winter monsoon, which strongly influences surface wind strength, was substantially greater during the last glacial period than in the Holocene, favoring maximum dune activity around the Last Glacial Maximum (*18*, *33*). Compared to its remarkable decline since the last deglaciation (*33*), variations of winter monsoon strength within the Holocene were relatively small. Two proxy records (*45*, *46*) do indicate higher strength in the Early Holocene (Fig. 3C), which might partially explain slow and gradual stabilization at some sites (e.g., SGD and ZBT) in response to rising precipitation at that time. However, the weaker winter monsoon reconstructed for the Late Holocene (Fig. 3C) cannot explain Late Holocene reactivation, which is more likely due to decreasing precipitation, a trend that is well supported by paleoclimatic data. In addition, the Dali Lake record from within the dune field (*47*) indicates water level drops in response to decreasing precipitation after about 5 ka ago (Fig. 1B).

The present environment of these dune fields is influenced by various human activities including grazing, farming, and, more recently, vegetation rehabilitation programs (*48*). Such human forcing likely played a role in shaping dune field stability in the past, too. Substantial human remains have been found in the dune fields as evidence of earlier human occupation since the Neolithic (*17*, *22*, *49*), but recent studies found that human habitation in this area was strongly influenced by climate change during prehistoric time (*49*). The Middle to Late Holocene climate transition toward aridification forced Late Neolithic inhabitants to develop subsistence strategies better adapted to drier conditions (*49*) or even abandonment and out-migration due to irreversible environmental change (*50*), resulting in the decline of Late Neolithic cultures in the deserts of northern China (*19*, *49*). Nevertheless, there is consensus that notable human influence on the dune field environment mainly occurred after about 2 ka ago (*17*, *22*), when human population increased. Clear evidence from historical documents has shown that excessive removal of vegetation coupled with droughts may lead to reactivation of dunes (*22*). The existing evidence indicates that changes in the extent of dune activity and bistability during the Early to Middle Holocene and much of the Late Holocene have been determined largely by monsoon variations, but human forcing factors likely accelerated transitions from vegetation-stabilized to active dune states in the Chinese dune fields after 2 ka ago.

As a radical modification to earlier interpretations, we propose that the gradual regional-scale response to Holocene variation of the monsoon climate does not reflect a simple linear response of vegetation to moisture availability, so that the area of stabilized dunes progressively expanded or shrank along well-established climatic gradients. Instead, this gradual landscape response reflects heterogeneity and a low level of connectivity among local dune systems—each with its own nonlinear behavior—as the monsoon climate changed through the Holocene. On a local level, ecological systems with intrinsic thresholds can have tipping points of their own (*2*), especially within a larger landscape with high diversity of land cover (*11*, *51*). Thus, the dunes can shift between active and vegetation-stabilized states at different values of the overall control parameters and initial conditions and at different times (Fig. 2). This heterogeneity in dune responses may be related to variations in sand grain size, dune area, local groundwater hydrology, the distribution of plant species effective in stabilizing dunes under a certain set of conditions, or many other factors. It may also reflect the history of a particular site and its surroundings. On a local level, dunes may have been persistently active because of a history of anthropogenic disturbance, or unusually well vegetated because of local high rainfall events, for example. Such perturbations are generally spatially and temporally diverse at multiple scales and have a stochastic component. If its components are spatially heterogeneous and weakly connected, the response of

the spatially distributed dune field system as a whole would consist of many asynchronous local shifts, and a smoothed response of the whole system instead of catastrophic shifts would be expected (*14*).

The apparent region-wide hysteresis indicated by differing paths of Early Holocene stabilization and Late Holocene reactivation of the Chinese dune fields (Fig. 3D) is particularly interesting in this context. The hysteresis in regional response may result from processes at multiple scales. At the local scale, the dynamics discussed by Yizhaq *et al.* (*5*, *6*) imply the persistence of an active dune state until precipitation reaches a value well above the threshold for the stabilized to active transition. Similar local hysteresis could also be related to some of the other biogeomorphic feedbacks proposed above. Even with substantial local heterogeneity in thresholds and timing of transitions, the general effect could be the observed regional-scale hysteresis. Greater human disturbance in the Late Holocene cannot explain the inferred hysteresis, which involves greater area of stable dunes after 2 ka ago than in the Early Holocene, at the same precipitation level (Fig. 3D).

The results of our analysis of critical transitions over the past 12,000 years have clear implications for understanding and predicting environmental change in the dune fields of northern China today, under the influence of both climate change and changing human land use. Transitions occurring at present and in the near future may appear gradual and smooth at the regional scale, but we should not be surprised to witness persistence of bistability and abrupt transitions of dune states at the local scale. Furthermore, the path of vegetation recovery and dune stabilization may be far from the path of earlier collapse at multiple temporal and spatial scales (*52*). The lagged response of dune field activity in northern China despite steep declines in wind speed in recent decades (*48*) might be attributable to such hysteresis. While these phenomena add considerable complexity and uncertainty, recent modeling studies also show that the geodiversity of dryland ecosystems constitutes an important factor in their vulnerability to climate change and anthropogenic disturbances (*51*). Our results also suggest that analysis over multiple spatial scales may provide new insight into the nature of Holocene landscape change in other regions, e.g., the collapse of the "Green Sahara."

Our results also have highly interesting implications regarding the complexity of the dune record as a paleoclimatic archive. On the basis of our reconstruction and model results, it is clear that in the study area, active dunes can exist under relatively wet conditions (precipitation as high as 600 mm), but some dunes can also remain stabilized even with precipitation less than 200 mm. Within this wide rainfall range for bistability, dunes can switch between the active and stabilized states triggered by local perturbations. Paleosols in these dune fields may ultimately provide more specific paleoclimatic information, e.g., from the stable isotopic composition of their organic matter or other geochemical evidence. However, caution is needed in relating stratigraphic evidence of dune state shifts to climate change, considering the range of climatic conditions under which this may occur at the local scale and the evidence of hysteresis in response at the regional scale. The results of this study, together with other evidence of the heterogeneous nature of dune records (*28*–*31*), clearly imply that a small number of individual dune sections are not sufficient for regional climate and environmental reconstruction. A compilation of well-dated dune records with large spatial coverage and high temporal resolution presents a much clearer picture of dune field evolution, more useful for paleoclimate reconstruction, but also revealing more of the true complexity of dune field nonlinear dynamics (*32*).

Our results demonstrate that the coexistence of active and vegetation-stabilized dunes under nearly identical environmental conditions, as observed in modern cases and predicted by models of dune dynamics, was an important and persistent phenomenon in the geologic past. The evolution of semiarid dune fields in northern China throughout the Holocene was driven by changes in monsoon precipitation. However, under similar climatic forcing, the dunes at different locations underwent critical transitions between active and stabilized states with their own timing and patterns, suggesting strong spatial heterogeneity and sensitivity to initial states. The resulting system-wide response of the entire dune fields to changing precipitation was gradual, without the abrupt transitions recorded at local sites, although this gradual change followed different paths during periods of overall dune stabilization and activation. This study implies that asynchronous transitions triggered by similar forcing may be common at the local scale in other spatially extended heterogeneous systems.

MATERIALS AND METHODS

Site-specific reconstruction

We performed a comprehensive analysis of 144 sedimentary stratigraphic sections recording changes in dune activity at individual sites during the Holocene across the three dune fields (76 sites described in this paper and our previous study, and 68 studied by other researchers). These records were interpreted using a total of 531 independent age determinations on depositional strata (data file S2). Most ages were obtained using OSL dating, the most widely applied method for dating dune records (*32*). By measuring the luminescence signal that accumulates over time following deposition of the sand grains, OSL dating determines the depositional age of the dune sand or sandy soil. The procedures are described in the original publications (data file S1), or for newly reported ages, follow Xu *et al.* (*18*, *33*, *53*). In developing this new dataset, we used applicable high-quality dune chronological data from the INQUA (International Union for Quaternary Research) Dunes Atlas chronologic dataset (*32*).

A new site-specific approach was applied in this study to synthesize chronologies at the dune field scale. We first reconstructed the dune state (active or stabilized) over time at individual sites based on the ages available from each section and evidence of soil formation (stability) or aeolian sand deposition (activity) (fig. S1) and then calculated the relative percentage of active and stabilized dunes in each time interval across all sites (fig. S2). At each site, we constructed linear age-depth models and calculated the sedimentation rate using site-specific age control. The sections were then divided into two groups based on each age-depth model. Sections with relatively consistent sedimentation rates, no apparent hiatuses, and good age-depth relationship ($R^2 > 0.9$) are referred to here as accumulative. In total, 29 sections were identified as accumulative and labeled as "A" in data file S1. The remaining 115 dune sections with either large changes in sedimentation rate or clear hiatuses are considered discontinuous and labeled as "D" in data file S1. Those include some sites with almost instantaneously deposited thick sand units [e.g., HK (Hekou), 207 Road-116 km, and ARA]. The larger number of discontinuous sections reflect the nature of dune field environments with frequent erosion and sediment reworking. The timing of sand deposition and soil formation in the accumulative sections was calculated by linear interpolation based on their age-depth models. Magnetic susceptibility of the sediments, which is proportional to the degree of pedogenesis,

was used as the indicator of shifts in local activity/stability for four accumulative sections. For discontinuous sections where erosional truncations or age jumps were identified, the OSL ages from sand units were used to indicate the time of sand deposition associated with dune activity. Paleosol ages are interpreted as recording the general time of dune stability and pedogenesis, based on the following reasoning. Thick, well-preserved paleosols in the dune fields of northern China are commonly interpreted as accretionary soils (*23*, *25*, *26*), in which frequent minor deposition of aeolian sand and dust occurred during soil formation on a vegetated surface, slowly building the soil upward over time. This process is especially likely in a persistent patchwork of stable and active dunes. If OSL ages within such an accretionary soil record the time of aeolian deposition, then we would expect systematically younger ages moving upward through the paleosol (*54*). That pattern is observed at sites in dune fields of northern China where paleosols were intensively dated [e.g., HK, XZB (Xinzhen Bei), NMD (Naiman Dong), WNTE (Wengniute East)]. Ages from the lowest parts of paleosols at some sites (e.g., HK) approach that of underlying sand and likely approximate the time of transition from activity to stability (*53*). The progressively younger ages higher in the paleosol should then fall within the time of soil formation. Alternatively, younger ages within the paleosols could possibly result from light exposure through bioturbation (*54*, *55*). In that case, OSL ages within the paleosol still likely fall within the period of stability that it represents, assuming that bioturbation occurred mainly before the soil's burial, when it was forming at the land surface under vegetation cover. The first sand age above a paleosol provides a minimum estimate for the return to dune activity at a site. We combined site-specific reconstructions to assess the overall pattern of temporal change in dune field activity (Fig. 2A). The relative proportion of sites recording sand deposition or soil development in each time interval (listed in data file S3) was then calculated and considered an approximate estimate of the relative extent of active or vegetation-stabilized dunes through time.

This approach may at least partially avoid the problems that might arise from different sampling strategies and intensity for dating at individual sites (*56*) because it does not rely on clustering in time of individual OSL ages. The full sequence of shifts between stabilized and active states is not recorded at all sites because of differences in preservation, but the alternations between soil formation and accumulation of unaltered aeolian sand recorded at each site indicate the minimum number of stabilized/active alternations that occurred there. A regional synthesis from this large dataset is likely to at least roughly represent changing proportions of active and stabilized surfaces in the study area.

Temporal resolution and uncertainties

A time interval of 500 years was used for 6 to 0 ka ago, and an interval of 1000 years was used for 12 to 6 ka ago. These interval sizes were chosen following simulations designed to estimate uncertainty in the percentage of sites with stabilized dunes in each interval, based on the errors of the underlying OSL ages. It is the inferred dune state (active or stabilized) at a given site that is assigned to each interval, not individual OSL ages, and more than one age supports the age assignment of many inferred episodes of stability or activity. However, we made the simplifying and generally conservative assumption that the probability an episode is incorrectly assigned to a time interval can be estimated from the probability distributions of individual OSL ages in the same time interval. With that assumption, we used 10,000 stochastically varying simulations of the distribution of stable and active sites over the past 12,000 years to estimate the uncertainty of our reconstruction.

Estimation of error in calculating percent stable sites over time

Each stratigraphic section used in this study was interpreted as recording one or more time intervals in which aeolian sand was active or stable at that location. The basis for making these interpretations is described in the article text. Each interval of stability or activity was assigned to 1 of 20 age classes or bins covering the time from 0 to 12,000 years ago, with 500-year bins from 0 to 6000 years ago and 1000-year bins from 6000 to 12,000 years ago. Assignment to bins was based on one or more numerical ages, mostly determined by the OSL method. Each age has 1σ errors calculated by standard methods.

Because of errors in dating, there is some uncertainty about the bin to which each activity/stability interval (A/S interval) belongs, and this, in turn, results in uncertainty in the percentage of stable sites over time. To estimate that uncertainty, we used a simulation method. To simplify the problem, we assumed that the bin assignment of an individual A/S interval at one site was determined by one numerical age, which has errors typical of numerical ages in that bin. Using that assumption, the probability that an individual A/S interval actually belongs in a younger or older bin can be estimated. This is generally a conservative assumption since the bin assignments constrained by two or more ages are less likely to be in error than those based on only one age.

All numerical ages used in the study were placed in the same age bins used for A/S intervals. We also used the relatively abundant available ages falling in two additional 1000-year bins back to 14 ka ago (the purpose of this "buffer" of older bins is explained below). For each bin, we calculated the average age and average 1σ error (the average age was generally very close to the bin midpoint). These values were then used as mean and SD parameters of a cumulative normal distribution, and the values of that distribution corresponding to boundaries of the four older and four younger bins were calculated. Those values were used to define the probabilities that an A/S interval in that bin actually falls within one of the four older or younger bins. With that information, we simulated 10,000 randomly varying distributions of A/S intervals across the 20 bins. In each iteration, each A/S interval in each bin was either left in that bin or shifted to older or younger ones based on comparing a random number (uniformly distributed, 0 to 1) to values of the cumulative normal distribution corresponding to bin boundaries. For example, in the 3.5- to 4-ka-ago bin, a random number between 0.000009 and 0.006608 would shift an A/S interval to the 2.5- to 3-ka-ago bin, but that happened very infrequently because of the low probability of random numbers falling within that narrow range; on the other hand, the many random numbers falling between ~0.25 and ~0.88 resulted in no shift. A/S intervals were not allowed to shift below the youngest bin or above 14 ka ago. The effect of this rule is small because (i) the probability of any shift is small in the youngest bins, and (ii) the two bins added at the old end of the range for the simulations act as a buffer reducing the upper boundary effect.

For each of the 10,000 iterations, the percentage of stable intervals relative to total intervals in a bin was calculated. For each bin, we then calculated the 2.5 and 97.5 percentiles of the 10,000 values of percent stable and used those to define likely errors for percent

stable, as shown in Fig. 3. Although the probabilities of an A/S interval shifting to older or younger bins are symmetrical, the central 95% of the simulated percent stable values sometimes have a skewed distribution, leading to asymmetrical error bars in Fig. 3. This is most pronounced for bins in which almost all sites are either stable or active, and most simulated values of percent stable are near 100% or 0%, with a tail extending to lower or higher values. Some asymmetry is also evident where the number of all sites or of stable or active sites drops off or increases steeply between bins. We believe both these effects are realistic representations of the probability distribution of percent stable in those contexts; for example, few active intervals are inferred for three bins in the Middle Holocene, so even with random shifts in the simulations, most iterations yield 90 to 100% stable in these bins.

Paleoclimate reconstruction data

Precipitation and wind strength are two important climatic factors affecting dune activity in northern China. A recent pollen-based reconstruction from Gonghai Lake is one of the most precise, quantitative precipitation records (*21*) and was used as representative of the large-scale precipitation in northern China. This record is from a site where modern annual precipitation (~445 mm) is similar to the southeast part of the dune fields. We used this record to represent Holocene precipitation variations in the study area, in comparison with other independent records (e.g., speleothem, loess, and lake level). Note that the wide range of reconstructed precipitation (300 to 600 mm) refers in particular to the estimated annual precipitation at the southeast margin of the dune fields. While there have been many reconstructions of Asian summer and winter monsoon circulations during the Holocene based on proxy records, quantitative reconstructions of wind strength are rare. This study referred to two qualitative records of the strength of the East Asian winter monsoon (EAWM), the predominant control on the strength of sand-transporting winds in the study area (*48*). One is a diatom record (*46*) in which the higher/lower inverse ratio between the relative abundance of two species, i.e., *Aulacoseira granulate* and *Cyclotella stelligera* (AG/CS), represents a stronger/weaker EAWM. Another EAWM index is based on a reconstruction of the thermal gradient in the northern South China Sea (*45*). The differences in the temperatures between the surface (or mixed-layer) water and thermocline (ΔT) are strongly modulated by the intensity of the EAWM. A lower/higher ΔT suggests a stronger/weaker mixing and, hence, indicates a stronger/weaker EAWM wind intensity.

Paleoclimate model simulations

To understand the response of the various dune fields studied here, it is helpful to also have spatially explicit information about the evolution of climate conditions. Reconstructions of past precipitation are only available from one location, but if the spatial gradient of precipitation throughout the Holocene was similar to that observed today (increasing from northwest to southeast; Fig. 1B), then we can assume that the temporal evolution of precipitation was similar in form at all study sites. To check whether that assumption is reasonable, we analyzed the results of a Holocene simulation from a complex Earth system model, MPI-ESM (*57*), covering the period from 8000 years before present to the present and including best estimates of all relevant climate forcings (most importantly, orbital forcing and volcanic eruptions). For comparison, the results from the TraCE-21 ka (CCSM3) model (*58*) that simulates annual precipitation throughout the Holocene were also analyzed (Fig. 3B). Results from MPI-ESM shown in Fig. 1 (E to G) indicate a northwest-southeast gradient of precipitation across the dune systems analyzed in this study throughout the past 8000 years, similar to that observed today, with all dune systems receiving progressively less precipitation in the Late Holocene as the Asian summer monsoon weakened in response to decreasing summer insolation. In the following, we therefore used the pollen reconstruction from Gonghai Lake as a proxy for precipitation changes at all sites. Note that the simulated precipitation is larger than the reconstruction, although they follow similar decreasing trends in the Late Holocene.

SUPPLEMENTARY MATERIALS

Supplementary material for this article is available at http://advances.sciencemag.org/cgi/content/full/6/9/eaay8020/DC1

Fig. S1. Typical dune stratigraphic sections at individual sites from the dune fields of northern China.

Fig. S2. Coexisting active and stabilized dunes in northern China during the past 12,000 years.

Data file S1. List of study sites from the dune fields of northern China.

Data file S2. Dataset of dune chronologies in the dune fields of northern China.

Data file S3. The sites where sand deposition or soil development is recorded during each time interval of the past 12,000 years.

REFERENCES AND NOTES

1. T. M. Lenton, H. Held, E. Kriegler, J. W. Hall, W. Lucht, S. Rahmstorf, H. J. Schellnhuber, Tipping elements in the Earth's climate system. *Proc. Natl. Acad. Sci. U.S.A.* **105**, 1786–1793 (2008).
2. M. Scheffer, S. Carpenter, J. A. Foley, C. Folke, B. Walker, Catastrophic shifts in ecosystems. *Nature* **413**, 591–596 (2001).
3. O. D. Vinent, L. J. Moore, Barrier island bistability induced by biophysical interactions. *Nat. Clim. Chang.* **5**, 158–162 (2015).
4. H. Tsoar, Critical environments: Sand dunes and climate change, in *Treatise on Geomorphology, Aeolian Geomorphology*, J. F. Shroder, N. Lancaster, D. J. Sherman, A. C. W. Baas, Eds. (Academic Press, 2013), vol. 11, pp. 414–427.
5. H. Yizhaq, Y. Ashkenazy, H. Tsoar, Why do active and stabilized dunes coexist under the same climatic conditions? *Phys. Rev. Lett.* **98**, 188001 (2007).
6. H. Yizhaq, Y. Ashkenazy, H. Tsoar, Sand dune dynamics and climate change: A modeling approach. *J. Geophys. Res.* **114**, F01023 (2009).
7. P. DeMenocal, J. Ortiz, T. Guilderson, J. Adkins, M. Sarnthein, L. Baker, M. Yarusinsky, Abrupt onset and termination of the African humid period: Rapid climate responses to gradual insolation forcing. *Quat. Sci. Rev.* **19**, 347–361 (2000).
8. V. Brovkin, M. Claussen, V. Petoukhov, A. Ganopolski, On the stability of the atmosphere vegetation system in the Sahara/Sahel region. *J. Geophys. Res.* **103**, 31613–31624 (1998).
9. T. M. Shanahan, N. P. McKay, K. A. Hughen, J. T. Overpeck, B. Otto-Bliesner, C. W. Heil, J. King, C. A. Scholz, J. Peck, The time-transgressive termination of the African humid period. *Nat. Geosci.* **8**, 140–144 (2015).
10. S. Kröpelin, D. Verschuren, A.-M. Lézine, H. Eggermont, C. Cocquyt, P. Francus, J.-P. Cazet, M. Fagot, B. Rumes, J. M. Russell, F. Darius, D. J. Conley, M. Schuster, H. von Suchodoletz, D. R. Engstrom, Climate-driven ecosystem succession in the Sahara: The past 6000 years. *Science* **320**, 765–768 (2008).
11. M. Claussen, S. Bathiany, V. Brovkin, T. Kleinen, Simulated climate–vegetation interaction in semi-arid regions affected by plant diversity. *Nat. Geosci.* **6**, 954–958 (2013).
12. Z. Liu, Y. Wang, R. Gallimore, M. Notaro, I. C. Prentice, On the cause of abrupt vegetation in North Africa during the Holocene: Climate variability vs. vegetation feedback. *Geophys. Res. Lett.* **33**, L22709 (2006).
13. S. Bathiany, M. Claussen, K. Fraedrich, Implications of climate variability for the detection of multiple equilibria and for rapid transitions in the atmosphere-vegetation system. *Clim. Dyn.* **38**, 1775–1790 (2012).
14. E. H. van Nes, M. Scheffer, Implications of spatial heterogeneity for catastrophic regime shifts in ecosystems. *Ecology* **86**, 1797–1807 (2005).
15. C. Xu, E. H. van Nes, M. Holmgren, S. Kéfi, M. Scheffer, Local facilitation may cause tipping points on a landscape level preceded by early-warning indicators. *Am. Nat.* **186**, E81–E89 (2015).
16. M. Holmgren, M. Hirota, E. H. van Nes, M. Scheffer, Effects of inter-annual climate variability on tropical tree cover. *Nat. Clim. Chang.* **3**, 755–758 (2013).
17. H. Lu, S. Yi, Z. Xu, Y. Zhou, L. Zeng, F. Zhu, F. Han, L. Dong, H. Zhuo, K. Yu, J. A. Mason, X. Wang, Y. Chen, Q. Lu, B. Wu, Z. Dong, J. Qu, X. Wang, Z. Guo, Chinese deserts

and sand fields in Last Glacial Maximum and Holocene Optimum. *Chin. Sci. Bull.* **58**, 2775–2783 (2013).
18. Z. Xu, H. Lu, S. Yi, J. Vandenberghe, J. A. Mason, Y. Zhou, X. Wang, Climate-driven changes to dune activity during the Last Glacial Maximum and deglaciation in the Mu Us dune field, north-central China. *Earth Planet. Sci. Lett.* **427**, 149–159 (2015).
19. Y. Wang, H. Cheng, R. L. Edwards, T. Q. He, X. G. Kong, Z. S. An, J. Y. Wu, M. J. Kelly, C. A. Dykoski, X. D. Li, The Holocene Asian monsoon: Links to solar changes and North Atlantic climate. *Science* **308**, 854–857 (2005).
20. H. Lu, S. Yi, Z. Liu, J. A. Mason, D. Jiang, J. Cheng, T. Stevens, Z. Xu, E. Lou, L. Jin, Z. Zhang, Z. Guo, Y. Wang, B. Otto-Bliesner, Variation of East Asian monsoon precipitation during the past 21 k.y. and potential CO_2 forcing. *Geology* **41**, 1023–1026 (2013).
21. F. Chen, Q. Xu, J. Chen, H. J. B. Birks, J. Liu, S. Zhang, L. Jin, C. An, R. T. Telford, X. Cao, Z. Wang, X. Zhang, K. Selvaraj, H. Lu, Y. Li, Z. Zheng, H. Wang, A. Zhou, G. Dong, J. Zhang, X. Huang, J. Bloemendal, Z. Rao, East Asian summer monsoon precipitation variability since the last deglaciation. *Sci. Rep.* **5**, 11186 (2015).
22. J. Sun, Origin of eolian sand mobilization during the past 2300 years in the Mu Us desert, China. *Quat. Res.* **53**, 78–88 (2000).
23. J. Sun, S.-H. Li, P. Han, Y. Chen, Holocene environmental changes in the central Inner Mongolia, based on single-aliquot-quartz optical dating and multi-proxy study of dune sands. *Palaeogeogr. Palaeoclimatol. Palaeoecol.* **233**, 51–62 (2006).
24. J. A. Mason, H. Lu, Y. Zhou, X. Miao, J. B. Swinehart, Z. Liu, R. J. Goble, S. Yi, Dune mobility and aridity at the desert margin of northern China at a time of peak monsoon strength. *Geology* **37**, 947–950 (2009).
25. H. Lu, J. A. Mason, T. Stevens, Y. Zhou, S. Yi, X. Miao, Response of surface processes to climatic change in the dunefields and Loess Plateau of North China during the late Quaternary. *Earth Surf. Process. Landf.* **36**, 1590–1603 (2011).
26. L. Yang, T. Wang, J. Zhou, Z. Lai, H. Long, OSL chronology and possible forcing mechanisms of dune evolution in the Horqin dunefield in northern China since the Last Glacial Maximum. *Quat. Res.* **78**, 185–196 (2012).
27. X. Yang, P. Liang, D. Zhang, H. Li, P. Rioual, X. Wang, B. Xu, Z. Ma, Q. Liu, X. Ren, F. Hu, Y. He, G. Rao, N. Chen, Holocene aeolian stratigraphic sequences in the eastern portion of the desert belt (sand seas and sandy lands) in northern China and their palaeoenvironmental implications. *Sci. China Earth Sci.* **62**, 1302–1315 (2019).
28. R. M. Bailey, D. S. G. Thomas, A quantitative approach to understanding dated dune stratigraphies. *Earth Surf. Process. Landf.* **39**, 614–631 (2014).
29. M. W. Telfer, P. P. Hesse, M. Perez-Fernandez, R. M. Bailey, S. Bajkan, N. Lancaster, Morphodynamics, boundary conditions and pattern evolution within a vegetated linear dunefield. *Geomorphology* **290**, 85–100 (2017).
30. S. A. Wolfe, O. B. Lian, C. H. Hugenholtz, J. R. Riches, Holocene eolian sand deposition linked to climatic variability, Northern Great Plains, Canada. *Holocene* **27**, 579–593 (2017).
31. D. S. G. Thomas, R. M. Bailey, Analysis of late Quaternary dunefield development in Asia using the accumulation intensity model. *Aeolian Res.* **39**, 33–46 (2019).
32. N. Lancaster, S. Wolfe, D. Thomas, C. Bristow, O. Bubenzer, S. Burrough, G. Duller, A. Halfen, P. Hesse, J. Roskin, A. Singhvi, H. Tsoar, A. Tripaldi, X. Yang, M. Zárate, The INQUA Dunes Atlas chronologic database. *Quat. Int.* **410**, 3–10 (2016).
33. Z. Xu, T. Stevens, S. Yi, J. A. Mason, H. Lu, Seesaw pattern in dust accumulation on the Chinese Loess Plateau forced by late glacial shifts in the East Asian monsoon. *Geology* **46**, 871–874 (2018).
34. P. D'Odorico, K. Caylor, G. S. Okin, T. M. Scanlon, On soil moisture–vegetation feedbacks and their possible effects on the dynamics of dryland ecosystems. *J. Geophys. Res.* **112**, G04010 (2007).
35. J. M. Nield, A. C. W. Baas, The influence of different environmental and climatic conditions on vegetated aeolian dune landscape development and response. *Glob. Planet. Chang.* **64**, 76–92 (2008).
36. T. E. Barchyn, C. H. Hugenholtz, Predicting vegetation-stabilized dune field morphology. *Geophys. Res. Lett.* **39**, L17403 (2012).
37. J. Roskin, I. Katra, D. G. Blumberg, Late Holocene dune mobilizations in the northwestern Negev dunefield, Israel: A response to combined anthropogenic activity and short-term intensified windiness. *Quat. Int.* **303**, 10–23 (2013).
38. Y. Miao, H. Jin, J. Cui, Human activity accelerating the rapid desertification of the Mu Us Sandy Lands, North China. *Sci. Rep.* **6**, 23003 (2016).
39. H. Yizhaq, Y. Ashkenazy, Periodic temporal oscillations in biocrust-vegetation dynamics on sand dunes. *Aeolian Res.* **20**, 35–44 (2016).
40. W. H. Schlesinger, J. F. Reynolds, G. L. Cunningham, L. F. Huenneke, W. M. Jarrell, R. A. Virginia, W. G. Whitford, Biological feedbacks in global desertification. *Science* **247**, 1043–1048 (1990).
41. E. Meron, *Nonlinear Physics of Ecosystems* (CRC Press, Taylor & Francis Group, 2015).
42. O. Rozenstein, E. Zaady, I. Katra, A. Karnieli, J. Admowski, H. Yizhaq, The effect of sand grain size on the development of cyanobacterial biocrusts. *Aeolian Res.* **15**, 217–226 (2014).
43. S. M. Munson, J. Belnap, G. S. Okin, Responses of wind erosion to climate-induced vegetation changes on the Colorado Plateau. *Proc. Natl. Acad. Sci. U.S.A.* **108**, 3854–3859 (2011).
44. C. M. Werner, J. A. Mason, P. R. Hanson, Non-linear connections between dune activity and climate in the High Plains, Kansas and Oklahoma, USA. *Quat. Res.* **75**, 267–277 (2011).
45. S. Steinke, C. Glatz, M. Mohtadi, J. Groeneveld, Q. Li, Z. Jian, Past dynamics of the East Asian monsoon: No inverse behaviour between the summer and winter monsoon during the Holocene. *Glob. Planet. Chang.* **78**, 170–177 (2011).
46. L. Wang, J. Li, H. Lu, Z. Gu, P. Rioual, Q. Hao, A. W. Mackay, W. Jiang, B. Cai, B. Xu, J. Han, G. Chu, The East Asian winter monsoon over the last 15,000 years: Its links to high-latitudes and tropical climate systems and complex correlation to the summer monsoon. *Quat. Sci. Rev.* **32**, 131–142 (2012).
47. Y. Goldsmith, W. S. Broecker, H. Xu, P. J. Polissar, P. B. deMenocal, N. Porat, J. Lan, P. Cheng, W. Zhou, Z. An, Northward extent of East Asian monsoon covaries with intensity on orbital and millennial timescales. *Proc. Natl. Acad. Sci. U.S.A.* **114**, 1817–1821 (2017).
48. Z. Xu, R. Hu, K. Wang, J. A. Mason, S.-Y. Wu, H. Lu, Recent greening (1981-2013) in the Mu Us dune field, north-central china, and its potential causes. *Land Degrad. Dev.* **29**, 1509–1520 (2018).
49. L. Guo, S. Xiong, Z. Ding, G. Jin, J. Wu, W. Ye, Role of the mid-Holocene environmental transition in the decline of late Neolithic cultures in the deserts of NE China. *Quat. Sci. Rev.* **190**, 98–113 (2018).
50. X. Yang, L. A. Scuderi, X. Wang, L. J. Scuderi, D. Zhang, H. Li, S. Forman, Q. Xu, R. Wang, W. Huang, S. Yang, Groundwater sapping as the cause of irreversible desertification of Hunshandake Sandy Lands, Inner Mongolia, northern China. *Proc. Natl. Acad. Sci. U.S.A.* **112**, 702–706 (2015).
51. H. Yizhaq, I. Stavi, M. Shachak, G. Bel, Geodiversity increases ecosystem durability to prolonged droughts. *Ecol. Complex.* **31**, 96–103 (2017).
52. M. Holmgren, M. Scheffer, El Niño as a window of opportunity for the restoration of degraded arid ecosystems. *Ecosystems* **4**, 151–159 (2001).
53. Z. Xu, J. A. Mason, H. Lu, S. Yi, Y. Zhou, J. Wu, Z. Han, Crescentic dune migration and stabilization: Implications for interpreting paleo-dune deposits as paleoenvironmental records. *J. Geogr. Sci.* **27**, 1341–1358 (2017).
54. R. J. Goble, J. A. Mason, D. B. Loope, J. B. Swinehart, Optical and radiocarbon ages of stacked paleosols and dune sands in the Nebraska Sand Hills, USA. *Quat. Sci. Rev.* **23**, 1173–1182 (2004).
55. M. D. Bateman, C. H. Boulter, A. S. Carr, C. D. Frederick, D. Peter, M. Wilder, Preserving the paleoenvironmental record in Drylands: Bioturbation and its significance for luminescence-derived chronologies. *Sediment. Geol.* **195**, 5–19 (2007).
56. M. W. Telfer, D. S. G. Thomas, Late Quaternary linear dune accumulation and chronostratigraphy of the southwestern Kalahari: Implications for aeolian palaeoclimatic reconstructions and predictions of future dynamics. *Quat. Sci. Rev.* **26**, 2617–2630 (2007).
57. M. A. Giorgetta, J. Jungclaus, C. H. Reick, S. Legutke, J. Bader, M. Böttinger, V. Brovkin, T. Crueger, M. Esch, K. Fieg, K. Glushak, V. Gayler, H. Haak, H. Hollweg, T. Ilyina, S. Kinne, L. Kornblueh, D. Matei, T. Mauritsen, U. Mikolajewicz, W. Mueller, D. Notz, F. Pithan, T. Raddatz, S. Rast, R. Redler, E. Roeckner, H. Schmidt, R. Schnur, J. Segschneider, K. D. Six, M. Stockhause, C. Timmreck, J. Wegner, H. Widmann, K. Wieners, M. Claussen, J. Marotzke, B. Stevens, Climate and carbon cycle changes from 1850 to 2100 in MPI-ESM simulations for the coupled model intercomparison project phase 5. *J. Adv. Model Earth Syst.* **5**, 572–597 (2013).
58. Z. Liu, B. L. Otto-Bliesner, F. He, E. C. Brady, R. Tomas, P. U. Clark, A. E. Carlson, J. Lynch-Stieglitz, W. Curry, E. Brook, D. Erickson, R. Jacob, J. Kutzbach, J. Cheng, Transient simulation of last deglaciation with a new mechanism for Bolling-Allerod warming. *Science* **325**, 310–314 (2009).
59. J. Ma, L. Yue, L. Yang, L. Sun, Y. Xu, OSL dating of Holocene sequence and palaeoclimate change record in southeastern margin of Mu Us desert, North China. *Quat. Sci.* **31**, 120–129 (2011).
60. A. Berger, M.-F. Loutre, Q. Yin, Total irradiation during any time interval of the year using elliptic integrals. *Quat. Sci. Rev.* **29**, 1968–1982 (2010).

Acknowledgments: We thank the researchers and students in our group for help in the field and laboratory. Those scientists publishing original data integrated in our dune dataset are especially thanked: Z. He, S.-H. Li, B. Liu, X. Liu, H. Jin, R. Lu, L. Yue, J. Sun, L. Yang, X. Yang, H. Zhao, and other researchers. We are grateful to M. Claussen and A. Dallmeyer from the Max-Planck-Institute for Meteorology for making their Holocene simulation available. We are grateful to J. Ma for providing the original data for the JJ site. We also thank the reviewers for helpful and supportive comments. **Funding:** This study was supported by the National Key R&D Program of China (2016YFA0600503), the National Natural Science Foundation of China (nos. 41871012 and 31770512), the Fundamental Research Funds for the Central Universities of China (020814380112), the U.S. National Science Foundation (EAR-1920625), and the KNAW CEP

(530-6CDP13). **Author contributions:** H.L., J.A.M., and Z.X. designed the research. Z.X. performed the research and analyzed the data. S.Y. and Y.Z. conducted the OSL dating. S.B. and J.C. analyzed the data from paleoclimate model simulations. J.A.M. analyzed the age uncertainties. Z.X. wrote the paper with the help of all coauthors. All authors edited the manuscript. **Competing interests:** The authors declare that they have no competing interests. **Data and materials availability:** All data needed to evaluate the conclusions in the paper are present in the paper and/or the Supplementary Materials. Additional data related to this paper may be requested from the authors. Correspondence and requests for materials should be addressed to Z.X.

Submitted 23 July 2019
Accepted 6 December 2019
Published 26 February 2020
10.1126/sciadv.aay8020

Citation: Z. Xu, J. A. Mason, C. Xu, S. Yi, S. Bathiany, H. Yizhaq, Y. Zhou, J. Cheng, M. Holmgren, H. Lu, Critical transitions in Chinese dunes during the past 12,000 years. *Sci. Adv.* **6**, eaay8020 (2020).